AIAA JOURNAL
Vol. 33, No. 10, October 1995

Optimal Design of Composite Lifting Surface for Flutter Suppression with Piezoelectric Actuators

Changho Nam*
Hankuk Aviation University, Koyang 411-791, Republic of Korea
and
Youdan Kim†
Seoul National University, Seoul 151-742, Republic of Korea

This paper presents the optimal design of an active flutter suppression system for an adaptive composite lifting surface. Rayleigh–Ritz method is used to develop the equations of motion of a laminated plate–wing model with segmented piezoactuators. A state space aeroservoelastic mathematical model by rational function approximation (RFA) of the unsteady aerodynamic forces is derived. The minimum state method combined with the optimization technique is adapted for RFA. The linear quadratic regulator with output feedback is employed in active control of the system. The thickness and size of the piezoelectric actuators that affect the structural properties as well as the control characteristics are held constant. The optimal placement of piezoelectric actuators for flutter suppression subject to minimize the controller performance index is determined analytically by using the optimization technique. The results show the capability of piezoactuators for the control of wing flutter. Numerical simulations of a model with the optimal actuators placement show a substantial saving in control effort compared with the initial model.

Introduction

TO prevent the static and dynamic instability in a composite wing, we can passively or actively suppress the instability by a proper choice of ply orientation and actuating the control surface. Recently, the application of piezoelectric materials to structural control may provide a new dimension in design to eliminate the possibility of instability by changing wing configuration to cause lift distribution variation. There has been a considerable amount of research activity in using piezosensor/actuators for the vibration control of flexible structures. Since the piezoelectric materials exhibit elastic deformation in proportion to the magnitude of an applied electric field and transfer forces to the structure, piezoelectric materials that are bonded at proper locations of a base structure can be used as actuators.

An analytic model for an induced strain actuator coupled with beams and plates has been developed by many authors.[1–5] Recently, the static and dynamic aeroelastic behavior of a wing structure with piezoactuators has been studied. Ehlers and Weisshaar[6,7] showed the effects of the piezoelectric actuators on the static aeroelastic behavior such as lift effectiveness, divergence, and roll effectiveness. Crawley et al.[8] used the typical section to represent a wing model and performed an analytic study to find the optimal placement and thickness of a piezoactuator for camber or twist control. They also used the aeroelastic tailoring and structural optimization procedure (TSO) code to evaluate the static aeroelastic response of the adaptive wing. Lazarus et al.[9] showed the ability of both articulated control surfaces and piezoelectric actuators to control the dynamic aeroelastic systems. Scott and Weisshaar[10] also examined the capability for panel flutter suppression with piezoelectric actuators and shape memory alloy actuators. Hajela and Glowasky[11] conducted a parameter study to suppress supersonic panel flutter with piezoelectric actuators. They used optimization techniques to find the best configuration of panels for both structural weight reduction and maximum flutter speed. Heeg[12] conducted an experimental study for flutter suppression of a beam model and demonstrated the application of piezoelectric materials for flutter suppression, which is affixed to a flexible mount system.

This paper presents an aeroservoelastic design for flutter suppression using the piezoelectric materials as actuators. A general approach to the integration of structural design and active control design, called integrated aeroservoelastic design, was proposed by Zeiler and Weisshaar.[13] Dracopoulos and Öz[14] also conducted an integrated design for aeroelastic control of a rectangular laminated plate using two point forces as actuators. The optimization technique was used to find the optimal ply orientations of the laminate and the design airspeed subject to maximize the critical aeroelastic speed. The purpose of this paper is to design an active control system for flutter suppression of a composite plate–wing with segmented piezoelectric actuators. The optimal placement of piezoelectric actuators on the composite wing structure for the flutter suppression is investigated. The analysis of the laminated composite wing with segmented piezoelectric actuators is conducted by the Rayleigh–Ritz method. The active control system design for flutter suppression requires the equations of motion to be expressed in a linear time-invariant state space form. Therefore, it is necessary to approximate the unsteady aerodynamic forces in terms of rational functions of the Laplace variables. The doublet lattice method is used to compute unsteady aerodynamic forces at Mach number 0.7, which are approximated as the transfer functions of the Laplace variable by the minimum state method combined with an optimization technique. To design the control system, a linear quadratic regulator theory with output feedback is used. The feedback control gains are obtained by solving coupled nonlinear matrix equations via numerical optimization routines. Since aerodynamic states are excluded from the state for feedback purposes, the output feedback includes structural states only. The optimal placement of piezoactuators is determined by an optimization technique referred to as the sequential linear programming method. The objective function is the control system performance index, and the design variables are the locations of piezoelectric actuators.

Modeling of Wing Structures with Piezoelectric Elements

Forces and moments acting on the laminated composite plate with segmented piezoactuators are derived by the classical laminate

Received June 28, 1994; revision received March 23, 1995; accepted for publication March 23, 1995.

*Assistant Professor, Department of Aeronautical and Mechanical Engineering. Member AIAA.

†Assistant Professor, Department of Aerospace Engineering. Member AIAA.

plate theory. The stress-strain relations of a thin piezoelectric layer are

$$\begin{Bmatrix} \sigma_1 \\ \sigma_2 \\ \sigma_{12} \end{Bmatrix}_p = \begin{bmatrix} Q_{p11} & Q_{p12} & 0 \\ Q_{p12} & Q_{p22} & 0 \\ 0 & 0 & Q_{p66} \end{bmatrix} \left\{ \begin{Bmatrix} \epsilon_1 \\ \epsilon_2 \\ \gamma_{12} \end{Bmatrix} - \begin{Bmatrix} d_{31} \\ d_{32} \\ 0 \end{Bmatrix} e_3 \right\} \tag{1}$$

or

$$\{\sigma\}_p = [Q_p]\{\{\epsilon\} - \{\Lambda\}\} \tag{2}$$

where $[Q_p]$ is the stiffness matrix of piezoelectric layer, d_{ij} is the piezoelectric strain coefficient, and e_3 is the applied electric field. This equation is similar to a stress-strain equation with thermal effects considering the fact that the piezoelectric strain Λ has the same form as thermal strain $\{\alpha\}\Delta T$. In-plane forces and moments of a laminated plate, including the loads of the piezoactuators, are obtained by integrating the stresses over the ply thickness and can be expressed as follows[15,16]:

$$\{N\} = \int \{\sigma\}\,dz = [A]\{\epsilon\} + [B]\{\kappa\} - \{N_\Lambda\} \tag{3}$$

$$\{M\} = \int \{\sigma\} z\,dz = [B]\{\epsilon\} + [D]\{\kappa\} - \{M_\Lambda\} \tag{4}$$

where $\{\epsilon\}$ and $\{\kappa\}$ are the midplane strain and curvature, respectively; and $[A]$, $[D]$, and $[B]$ are extension, bending, and extension/bending coupling stiffness matrices, respectively. These matrices are influenced by not only the ply orientations of the laminate but also the geometry of the piezoactuators. In-plane forces and moments due to actuator strain are given by

$$\{N_\Lambda\} = \int_{zp} [Q_p]\{\Lambda\}\,dz \tag{5}$$

$$\{M_\Lambda\} = \int_{zp} [Q_p]\{\Lambda\} z\,dz \tag{6}$$

where z_p is the coordinate through thickness in the piezoelectric material.

The strain energy of plate with piezoelectric material can be expressed as

$$U = \frac{1}{2}\iint_{A,Ap} \lfloor \epsilon \ \kappa \rfloor \begin{bmatrix} A & B \\ B & D \end{bmatrix} \begin{Bmatrix} \epsilon \\ \kappa \end{Bmatrix} dx\,dy - \iint_{Ap} \lfloor N_\Lambda \ M_\Lambda \rfloor \begin{Bmatrix} \epsilon \\ \kappa \end{Bmatrix} dx\,dy \tag{7}$$

The kinetic energy is

$$T = \frac{1}{2}\iint_{A,Ap} \rho(\dot{u}^2 + \dot{v}^2 + \dot{w}^2)\,dx\,dy \tag{8}$$

where A and A_p represent the area of the composite plate and piezoelectric material, respectively; u, v, and w are displacements in the x, y, and z directions, respectively. These energies are the functions of the ply orientations of the laminate and the piezoelectric parameters, which are the actuator thickness, area, and locations.

It is impossible to obtain closed-form solutions to the laminated plate due to the complexity of the equation, the arbitrary boundary conditions, and external forces such as unsteady aerodynamic forces. In this study, the Rayleigh–Ritz method, which is faster and has the same accuracy as the finite element method, is adopted for the structural analysis. To apply the Rayleigh–Ritz method, we introduce displacement functions in the generalized coordinate system to represent displacements u, v, and w,

$$u(x, y, t) = \sum_{i=1}^{l} X_i(x, y) q_i(t) \tag{9a}$$

$$v(x, y, t) = \sum_{j=l+1}^{l+m} Y_j(x, y) q_j(t) \tag{9b}$$

$$w(x, y, t) = \sum_{k=l+m+1}^{l+m+n} Z_k(x, y) q_k(t) \tag{9c}$$

where $X(x, y)$, $Y(x, y)$, and $Z(x, y)$ are shape functions that must be properly chosen so as to satisfy the geometric boundary conditions of the wing structures. Using these displacement expressions, equations for strain energy and kinetic energy are written in matrix form,

$$U = \tfrac{1}{2}\{q\}^T[K_s]\{q\} - \lfloor Q_\Lambda \rfloor\{q\} \tag{10}$$

$$T = \tfrac{1}{2}\{\dot{q}\}^T[M_s]\{\dot{q}\} \tag{11}$$

where $\lfloor Q_\Lambda \rfloor$ is the control force vector due to the actuation strain.

For the design of the suppression system of a symmetric laminated plate model with piezoelectric actuators, the model is assumed to have the surface bonded piezoelectric actuators on the opposite side of the plate at the same location. It is also assumed that the same magnitude but the opposite direction of electric field is applied to the actuator so as to create a pure bending moment for flutter suppression as shown in Fig. 1a. With these assumptions, the displacements in the x and y directions can be neglected. To express the displacement in the z direction, we used the free-free beam vibration modes in the x direction (chordwise direction) and the cantilever beam vibration modes in the y direction (spanwise direction) as follows:

$$Z_k(x, y) = \Phi_i(x)\Psi_j(y) \tag{12}$$

$$\begin{aligned} \Phi_i(x) &: 1, && i = 1 \\ &: \sqrt{3}\left(1 - 2\frac{x}{c}\right), && i = 2 \\ &: \left(\cos\alpha_i\frac{x}{c} + \cosh\alpha_i\frac{x}{c}\right) \\ &\quad - \beta_i\left(\sin\alpha_i\frac{x}{c} + \sinh\alpha_i\frac{x}{c}\right), && i = 3, 4, 5, \ldots \end{aligned} \tag{13}$$

$$\begin{aligned} \Psi_j(y) &: \left(-\cos\bar{\alpha}_j\frac{y}{l} + \cosh\bar{\alpha}_j\frac{y}{l}\right) \\ &\quad + \bar{\beta}_j\left(-\sin\bar{\alpha}_j\frac{y}{l} + \sinh\bar{\alpha}_j\frac{y}{l}\right), && j = 1, 2, 3, \ldots \end{aligned} \tag{14}$$

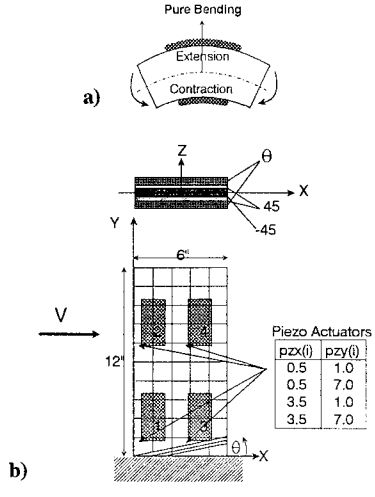

Fig. 1 a) Pure bending control by piezoactuators and b) composite plate wing model with piezoactuators.

In Eq. (10), if we express $\{Q_A\}$ in terms of the applied voltage $\{u\}$, it becomes as follows:

$$\{Q_A\} = \sum_{i=1}^{np} \frac{1}{t_p}\left\{\left(\frac{t_s}{2}+t_p\right)^2 - \left(\frac{t_s}{2}\right)^2\right\} \times \iint_{Ap_i} \left\{[Q_p]\begin{Bmatrix} d_{31} \\ d_{32} \\ 0 \end{Bmatrix}\right\}^T \{Z''\}\,dx\,dy\,V(i) = [F_p]\{u\} \tag{15}$$

where

$$\{Z''\}^T = -\left\lfloor \frac{\partial^2 Z}{\partial x^2}, \frac{\partial^2 Z}{\partial y^2}, 2\frac{\partial^2 Z}{\partial x \partial y}\right\rfloor \tag{16}$$

$$\{u\}^T = \lfloor V(1), V(2), \ldots, V(i), \ldots, V(np)\rfloor \tag{17}$$

where t_s and t_p are the thicknesses of the laminate and piezoelectric layer, respectively; $[F_p]$ is the control force per unit voltage; np is the number of bonded piezoelectric materials; and $V(i)$ is the applied voltage to the ith piezoelectric actuator.

Lagrange's equations result in a set of ordinary differential equations of motion as follows:

$$[M_s]\{\ddot{q}\} + [K_s]\{q\} = [F_p]\{u\} + \bar{q}[A]\{q\} \tag{18}$$

where $\bar{q}$ is the dynamic pressure, and $[A]$ is the unsteady aerodynamic force matrix. The aerodynamic force matrix is calculated using the doublet lattice method[17] for Mach 0.7 and 12 reduced frequencies ranging from 0 to 1.2. For calculation of the pressure distribution on an oscillating plate–wing undergoing simple harmonic motion, the plate model is divided into total 50 panels arranged in 10 spanwise direction and 5 chordwise direction. The terms $[M_s]$ and $[K_s]$ are, respectively, the generalized mass and stiffness matrices, including the effect of the piezoelectric actuators placement, and $[F_p]$ is the control force matrix due to unit applied electric field. After the vibration analysis, a model reduction is performed to obtain a set of equations of motion in the modal coordinates using the first six vibration modes.

Rational Function Approximation—Minimum State Method

The classical aeroelastic analysis such as the V-g method and p-k method is performed in the frequency domain using unsteady aerodynamic forces computed for simple harmonic motion. However, for the aeroservoelastic analysis and design, it is necessary to transform the equations of motion into the state space form. This requires one to approximate the unsteady aerodynamic forces in terms of rational functions of the Laplace variable. There are several methods for the rational function approximation (RFA) such as Roger's method, matrix Pade method, and minimum state method.[18] However, when the RFA is conducted, it causes an increase in the total number of states due to the number of augmented aerodynamic states to represent unsteady aerodynamic forces accurately. If an optimization technique is applied, the RFA can be improved without increasing the additional augmented aerodynamic states. In this paper, the minimum state method[19] combined with an optimization technique is adopted for the rational function approximation, since the increase in the size of the augmented aerodynamic state is smaller than any other methods.

The minimum state method[19] approximates the aerodynamic force matrix by

$$[A_{ap}(\bar{s})] = [A_0] + [A_1]\bar{s} + [A_2]\bar{s}^2 + [D'][\bar{s}I - R']^{-1}[E]\bar{s} \tag{19}$$

where $\bar{s}$ is the nondimensionalized Laplace variable ($\bar{s} = sb/V$), V is the airspeed, b is the semichord, and s is the Laplace variable. The components of diagonal matrix $[R']$ are negative constants that are selected arbitrarily. For a given $[R']$ matrix, $[A_0]$, $[A_1]$, $[A_2]$, $[D']$, and $[E]$ are determined by using repeated least-square fit. More details can be found in Refs. 18 and 19. The $[R']$ terms are chosen using an optimization technique that minimizes the least-square errors without an increase in additional aerodynamic lag terms. The Davidon–Fletcher–Powell method[20] is applied to minimize the overall least-square errors with components of the diagonal matrix $[R']$ as design variables. The objective function for the RFA is defined as

$$J = \sqrt{\sum_{l=1}^{nk}\left\{\frac{|[A(ik_l)] - [A_{ap}(ik_l)]|}{\max\{|[A(ik_l)]|,\ 1\}}\right\}^2} \tag{20}$$

where k is the reduced frequency ($k = \omega b/V$), $[A_{ap}]$ is the approximate value, and $[A]$ is the tabular value of the aerodynamic force matrix, respectively.

Using Eq. (19) for the RFA and the state vector $\{x\}^T = \lfloor q\ \dot{q}\ q_a\rfloor$, the linear time-invariant state space equations of motion that include the effects of piezoelectric control forces are expressed as follows:

$$\{\dot{x}\} = [F]\{x\} + [G]\{u\} \tag{21}$$

where

$$[F] = \begin{bmatrix} [0] & [I] & [0] \\ -[M]^{-1}[K] & -[M]^{-1}[B] & [M]^{-1}[D] \\ [0] & [E] & [R] \end{bmatrix} \tag{22}$$

$$[G] = \begin{bmatrix} [0] \\ [M]^{-1}[F_p] \\ [0] \end{bmatrix} \tag{23}$$

$$[M] = [M_s] - \tfrac{1}{2}\rho b^2[A_2] \tag{24}$$

$$[B] = -\tfrac{1}{2}\rho b V[A_1] \tag{25}$$

$$[K] = [K_s] - \tfrac{1}{2}\rho V^2[A_0] \tag{26}$$

$$[D] = \tfrac{1}{2}\rho V^2[D'] \tag{27}$$

$$[R] = \frac{V}{b}[R'] \tag{28}$$

where ρ is the air density. If $[R']$ is set to be a $m \times m$ matrix, the total number of states is $12 + m$.

Optimal Output Feedback Design

Since the system matrix is a function of the dynamic pressure, it is necessary to choose the design airspeed for designing the control system. By choosing the design air speed (V_{Design}), the linear quadratic regulator (LQR) with output feedback is applied for design of the flutter suppression system. The design procedure for LQR with output feedback is briefly summarized next. More detailed discussions can be found in Refs. 21–24. Consider a linear time-invariant system

$$\begin{aligned} \{\dot{x}\} &= [F]\{x\} + [G]\{u\} \\ \{y\} &= [H]\{x\} \end{aligned} \tag{29}$$

The output matrix $[H]$ is specified such that the aerodynamic states are excluded from the state for feedback purpose. The admissible controls are output feedback of the form

$$\{u\} = -[K_G]\{y\} \tag{30}$$

where $[K_G]$ is an output feedback gain matrix, which consists of constant coefficients to be determined by the design procedure. The performance index to be minimized is selected as follows:

$$J = \int_0^\infty [\{y\}^T[Q]\{y\} + \{u\}^T[R]\{u\}]\,dt \tag{31}$$

where $[Q] \geq 0$ and $[R] > 0$ are symmetric weighting matrices. Since the initial state $\{x_0\}$ may not be known, we adopt Levine and

Athans' procedure[21] that minimizes the expected value of performance index

$$\bar{J} = E\{J\} = \text{tr}\{[P][X_0]\} \tag{32}$$

where the operator $E\{\cdot\}$ denotes the expected value over all possible initial conditions, and $\text{tr}\{\cdot\}$ denotes the trace of a square matrix. The symmetric matrices P and X_0 are defined by

$$[X_0] = \{x_0\}\{x_0\}^T \tag{33}$$

$$[P] = \int_0^\infty e^{[F_c]^T t}[H]^T \left\{[Q] + [K_G]^T[R][K_G]\right\}[H]e^{[F_c]t}\,dt \tag{34}$$

where

$$[F_c] = [F] - [G][K_G][H] \tag{35}$$

The usual assumption is that the initial states are uniformly distributed on the unit sphere; then $[X_0]$ becomes an identity matrix. It is well known that matrix $[P]$ in Eq. (34) can be obtained by solving the following Lyapunov equation[25]:

$$[\Sigma] \equiv [F_c]^T[P] + [P][F_c] + [H]^T[Q][H] + [H]^T[K_G]^T[R][K_G][H] = [0] \tag{36}$$

Note that the Lyapunov equation is a symmetric linear matrix equation. The solution of the Lyapunov equation can be obtained directly by solving simultaneous linear equations[26]; however, this approach takes lots of computation time and storage. One of the most efficient and robust algorithms to solve Lyapunov equations uses quadratic regulator factorization.[27] In this algorithm, the Lyapunov equation is transformed into a simpler equation by use of Schur transformations.

Now, our problem is to determine the optimal output feedback gain matrix $[K_G]$ at the design speed, by minimizing Eq. (32) subject to the algebraic matrix constraint Eq. (36). The design speed, which is chosen arbitrarily, is usually larger than the open-loop flutter speed. To solve this problem with a constraint equation, a Lagrange multiplier approach[28] is widely used. The Hamiltonian is defined by adjoining the constraint Eq. (36) to the performance index Eq. (32) and expressed as follows:

$$\mathcal{H} = \text{tr}\{[P][X_0]\} + \text{tr}\{[\Sigma][S]\} \tag{37}$$

where $[S]$ is a symmetric matrix of Lagrange multipliers that still needs to be determined. The following conditions are necessary for $[P]$, $[S]$, and $[K_G]$ to be the extrema:

$$\frac{\partial \mathcal{H}}{\partial [P]} = [0], \qquad \frac{\partial \mathcal{H}}{\partial [S]} = [0], \qquad \frac{\partial \mathcal{H}}{\partial [K_G]} = [0] \tag{38}$$

Applying Eq. (38) to Eq. (37), necessary conditions for optimality are obtained as follows:

$$[F_c]^T[P] + [P][F_c] + [H]^T[Q][H] + [H]^T[K_G]^T[R][K_G][H] = [0] \tag{39}$$

$$[F_c][S] + [S][F_c]^T + [X_0] = [0] \tag{40}$$

$$[R][K_G][H][S][H]^T - [G]^T[P][S][H]^T = [0] \tag{41}$$

There exist several numerical approaches to solve Eqs. (39–41). Gradient-based routines[24] can be used with various optimization algorithms. Moerder and Calise[22] proposed an efficient iterative algorithm, which converges to a local minimum if the following conditions hold: 1) there exists an output gain matrix $[K_G]$ such that $[F_c]$ is stable, 2) the output matrix H has full row rank, 3) the control weighting matrix $[R]$ is positive definite, and 4) the output state weighting matrix $[Q]$ is positive semidefinite and should be chosen so that all unstable states are weighted in the performance index. The iterative algorithm for finding solution is outlined as follows:

Step 1: Choose $[K_G]$ such that $[F_c]$ in Eq. (35) has all of the eigenvalues with negative real parts.

Step 2: With given $[K_G]$ and the corresponding $[F_c]$, solve the Lyapunov Eqs. (39) and (40) for $[P]$ and $[S]$, and compute current performance index value $J = \text{tr}\{[P][X_0]\}$.

Step 3: Evaluate the gain update direction

$$\Delta[K_G] = [R]^{-1}[G]^T[P][S][H]^T([H][S][H]^T)^{-1} - [K_G] \tag{42}$$

Step 4: Update the gain by

$$[K_G]_{\text{new}} = [K_G] + \alpha\,\Delta[K_G] \tag{43}$$

where α is chosen so that the closed-loop system $[F_c]$ is asymptotically stable, and the performance index of the updated system is less than that of the current system. In this paper, α is set to be 0.3.

Step 5: Iterate steps 2–4 until the converged solution is obtained.

Any minimization algorithm requires the selection of an initial stabilizing gain. However, such a gain may or may not be easy to find. One possible way to find the initial gain matrix is to use root locus techniques by closing one loop at a time in the control system. In this study, first we solve the full state LQR problem with performance index Eq. (31) and construct the initial stabilizing output gain matrix by choosing the corresponding gain parameters to be used in the output feedback from the resulting LQR gain matrix elements.

Optimization Problem Formulation

The optimization technique is applied to determine the best locations of piezoelectric actuators for the design of an efficient flutter suppression system. The objective function is the performance index of the control system defined as Eq. (32). The formulation of this optimization problem may be stated as follows:

Find actuators locations

$$\boldsymbol{X}$$

to minimize

$$\bar{J} = \text{tr}\{[P][X_0]\}$$

subject to

$$g_j(\boldsymbol{X}) \le 0, \qquad j = 1, 2, \ldots, m \tag{44}$$

and

$$\boldsymbol{X}_l \le \boldsymbol{X} \le \boldsymbol{X}_u$$

where $\boldsymbol{X}$ is the design variables vector, and $\boldsymbol{X}_l$ and $\boldsymbol{X}_u$ are the lower and upper limit of design variables, respectively. The term g_j is the inequality constraint. A total of eight design variables $\boldsymbol{X}$ are considered in this study. These are x, y coordinates of the four piezoactuators, $pzx(i)$ and $pzy(i)$ shown in Fig. 1b. Eleven constraints are considered and defined as follows:

Five constraints on the closed-loop damping ratios:

$$\xi_i = -\frac{\bar{\sigma}_i}{\sqrt{\bar{\sigma}_i^2 + \bar{\omega}_i^2}} \ge \xi_{0i}, \qquad i = 1, 2, \ldots, 5 \tag{45}$$

where $\bar{\sigma}_i$ and $\bar{\omega}_i$ are the real and imaginary parts of the closed-loop eigenvalues. The first five eigenvalues of the closed loop are considered as the constraints.

Six constraints on the placement of four piezoactuators without overlapping:

$$pzx(i) - pzx(j) \ge 1.5 \quad \text{or} \quad pzy(i) - pzy(j) \ge 3.0, \qquad i, j = 1, 2, 3, 4 \tag{46}$$

There are also side constraints on design variables for the actuators to be placed within plate boundary.

The sequential linear programming (SLP) method[20] in the general purpose optimization program ADS[29] is used to solve this problem. In the SLP method, the nonlinear objective function and constraints are linearized by a first-order Taylor series expansion. The optimal design resulting from the approximate linear programming problem forms the initial point for the next iteration. The process is repeated

until prescribed convergence criteria are met. The move limit on design variables is needed to prevent unlimited moves as well as limit the design changes to the region of applicability of the approximation. The initial relative move limit is set to be 20% of the initial value of the design variables. The move limit is reduced to ensure convergence as the optimization progresses. The modified method of feasible directions is used to solve the direction finding subproblem, and the polynomial interpolation is used for the one-dimensional search. Any gradient information needed is calculated by the finite difference method using a 0.1% step.

Numerical Examples and Results

The plate model containing four sets of piezoelectric actuators is used as a model for the control system design (see Fig. 1b). It is assumed that a set of actuators is bonded on both top and bottom surfaces of the laminated plate to generate a pure bending force. The size of each piezoactuator is 1.5 × 3.0 in. The material properties used in this study are given in Table 1. The laminate has six symmetric layers, $[\theta/\pm 45]_s$. Each layer has a uniform thickness, which is 0.02 in., respectively. The initial coordinates of the piezoactuators are $pzx(i) = 0.5, 0.5, 3.5$, and 3.5 and $pzy(i) = 1.0, 7.0, 1.0$, and 7.0 as in Fig. 1b. The open-loop flutter speed is calculated by the V-g method and plotted against ply orientation in Fig. 2. It is seen that the flutter speed is low around 10- and 100-deg ply angles. The region between 0 and 90 deg of the ply orientation represents the wash-in, which twists to increase the angle of attack under loading and causes divergence at low dynamic pressure. The main purpose of this study is to design the control system for flutter suppression only. The $[105/\pm 45]_s$ wash-out wing model that has low flutter speed is taken as the base model for the suppression system design in the optimization study, and the wash-in wing model is not considered in this study. In the $[105/\pm 45]_s$ model, the flutter occurs at around 620 fps without a control system.

The open-loop flutter analysis of the $[105/\pm 45]_s$ laminate is conducted with the unsteady aerodynamics transformed into the Laplace domain through the minimum state method. The result is shown in Fig. 3. For the construction of Eq. (21), a total of six components of the $[R']$ matrix are used for the RFA. Therefore, the dimension of the state vector is 18. The optimized values of $[R']$ and the objective function defined as Eq. (20) are

$$[R'] = \text{diag}\{-0.0072, -0.048, -0.197, -0.49, -0.67, -0.98\}$$

and 1.621, respectively. As in Fig. 3, flutter occurs at 620 fps by the first torsion mode and flutter frequency is about 59 Hz.

Table 1 Material properties

Composite materials	Piezoelectric materials
$E_1 = 14.21 \times 10^6$ psi	$E_p = 9.137 \times 10^6$ psi
$E_2 = 1.146 \times 10^6$ psi	$\rho_p = 0.28$ lb/in.^{3}
$G_{12} = 0.8122 \times 10^6$ psi	$\nu_p = 0.3$
$\bar{\rho} = 0.05491$ lb/in^3.	$d_{31} = 6.5 \times 10^{-9}$ in./V
$\nu_{12} = 0.28$	$d_{32} = 6.5 \times 10^{-9}$ in./V

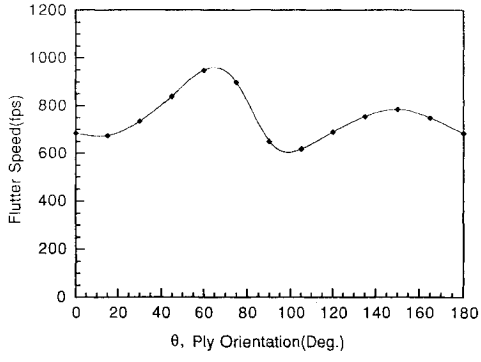

Fig. 2 Open-loop root loci for $[105/\pm 45]_s$ initial design.

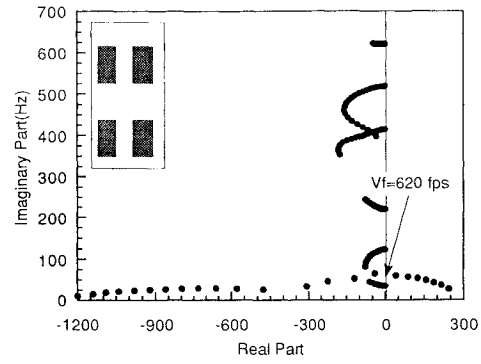

Fig. 3 Flutter speed variation with ply orientations of composite wing.

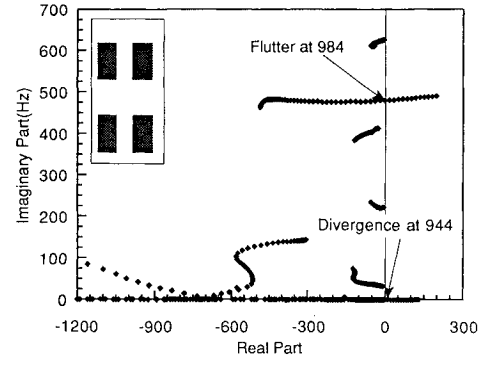

Fig. 4 Closed-loop root loci for $[105/\pm 45]_s$ initial design.

For the active control design, the design speed V_{Design} is set to be 800 fps, which is chosen arbitrarily. At the design speed, the open-loop system is unstable in the first torsion mode, yielding unstable eigenvalues at $159.3 \pm j304.1$. The open-loop matrix equation is supplemented with a control term. The control input $\{u\}$ is determined by LQR with output feedback subject to minimize the performance index at the design speed. To select the initial gain matrix, first we solve the full state LQR problem with performance index Eq. (31) and construct the initial stabilizing output gain matrix by choosing the corresponding gain parameters to be used in the output feedback from the resulting LQR gain matrix elements. For the full state LQR problem, the weighting matrices $[Q]$ and $[R]$ in Eq. (31) are set to be $50[I]$ and $[I]$, respectively. The loci of the closed-loop aeroelastic roots with increasing airspeed are plotted in Fig. 4. Above the design speed, the control law provides flutter mode control. The model is stable until a divergence occurs at about 944 fps. The performance index defined in Eq. (32) for the active control system is 6.26×10^6.

The optimization technique is applied to find the best locations of piezoelectric actuators for flutter suppression through the minimization of the performance index. The constraints on closed-loop damping ratios are reasonably set. These are

$$\xi_{0i} = 0.04, 0.03, 0.02, 0.01, 0.01 \qquad i = 1, 2, \ldots, 5 \qquad (47)$$

Figures 5 and 6 show the variations in the actuators locations and the objective function value during the optimization process. Note that the performance index value is increased after one iteration since the initial configuration violates the constraints on the damping ratios. As shown in Figs. 5 and 6, the optimization process tries to reduce the objective function value and moves the number 4 actuator to the tip. However, violation of constraints on the damping ratios forces the number 4 actuator back in the root direction, making the constraints active. This causes an increase in the objective function value. A trade off between the reduction of the performance index and the satisfaction of constraints in the optimization process is performed during the optimization process to determine the best locations of actuators. The final placements of the piezoactuators are $pzx(i) = 0.0, 0.42, 4.5$, and 2.54 and $pzy(i) = 0.0, 4.58, 0.0$, and 6.49. The actuators are moving to the locations to suppress the unstable flutter mode most effectively during the optimization

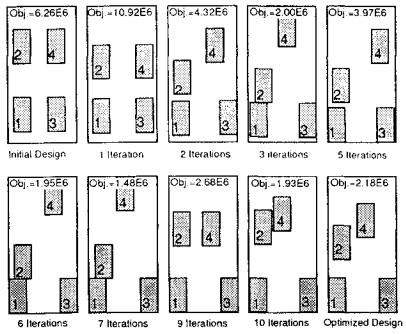

Fig. 5 Variation in piezoactuators placement during the optimization process.

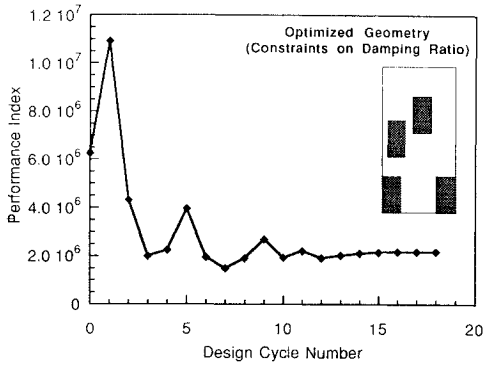

Fig. 6 Iteration histories of performance index.

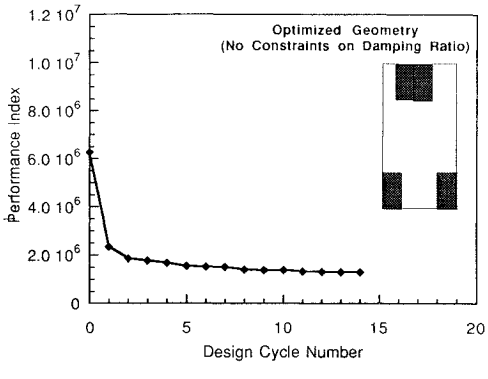

Fig. 7 Iteration histories of performance index without constraint on closed-loop damping ratio.

process. To create maximum torsional moment for the control, the actuators 1 and 3 are approaching the leading edge and the trailing edge of the root, respectively. This location is also good for the first bending mode control. Note that the $[105/\pm 45]_s$ wing model twists under the bending moment due to the bending/torsion coupling. The optimal value of the objective function that is the performance index is 2.18×10^6. There is a reduction in the performance index of about 65% from the initial value. From the calculation of deformation with a given constant voltage applied to the actuators, it was found that the wing model with the optimized actuator placements creates larger deflection and more camber to generate aerodynamic forces.

To see the effects of the damping ratio constraints on the actuators' placement, the optimization process is performed without the damping ratio constraints. Figure 7 shows the iteration histories of the performance index when the constraints on the closed-loop damping ratio are eliminated from the optimization formulation. The figure shows that the objective function rapidly converges to 1.32×10^6, which is a much smaller value than that when the damping ratio constraints are included. As shown in Fig. 7, number 2 and 4 actuators move to the tip region. The optimal placements of the piezoactuators are $pzx(i) = 0.0$, 1.04, 4.5, and 2.54 and $pzy(i) = 0.0$, 9.0, 0.0, and 9.0. The closed-loop damping ratios

Table 2 Comparison of the closed-loop damping ratios for each design

Initial design	Optimal design with constraints	Optimal design without constraints
0.352	0.389 (active)	0.367
0.025	0.029 (active)	0.026
0.873	0.845	0.832
0.025	0.029	0.029
0.051	0.051	0.051

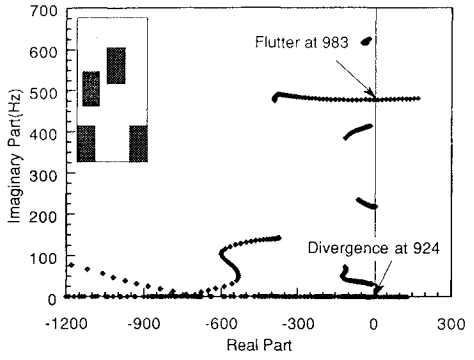

Fig. 8 Closed-loop root loci for $[105/\pm 45]_s$ optimized design.

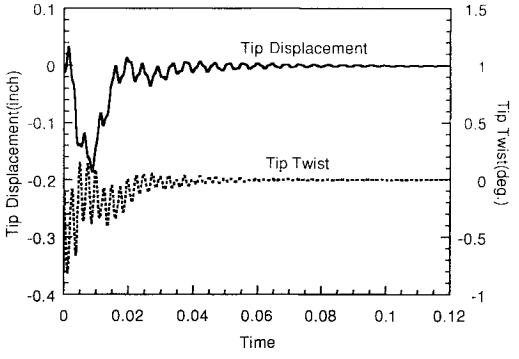

Fig. 9 Time histories of the model with initial piezoactuators placement.

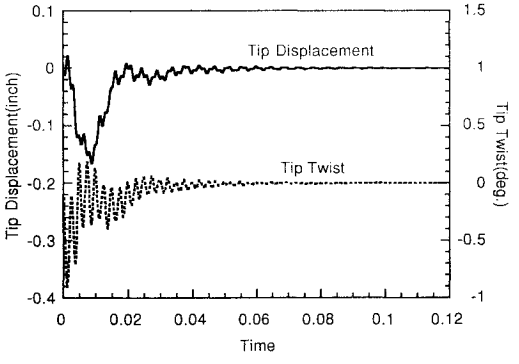

Fig. 10 Time histories of the model with optimal piezoactuators placement.

for each design are presented in Table 2 for comparison. It can be seen that the closed-loop damping ratios of first two modes are active when the damping ratios are included as constraints in the optimization.

Figure 8 shows the closed-loop root loci about the optimized geometry. The system is stable until a divergence occurs about 924 fps. The results of the root loci about the optimized geometry are very similar to those of the initial geometry. To compare the performance of the control systems, the responses and the control voltages applied to the piezoactuators at the design speed are simulated for each geometry. Figures 9 and 10 show the time histories of tip displacement and twist at the midchord in the model with initial

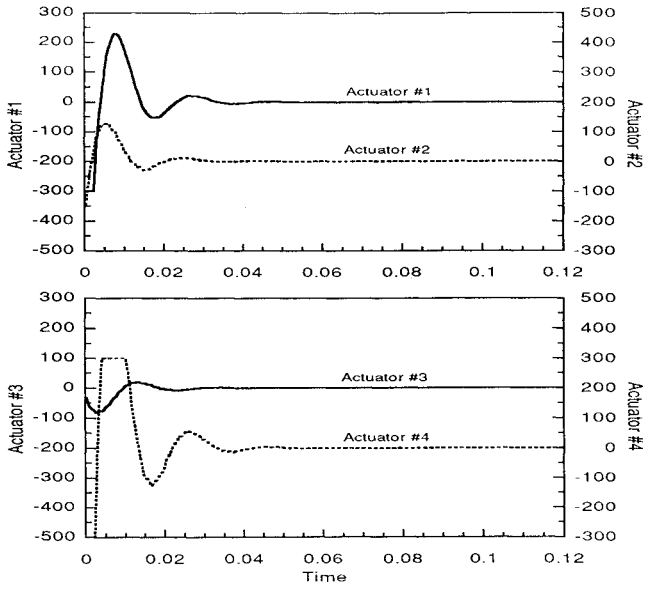

Fig. 11 Control voltages applied to the piezoelectric actuators of the initial design.

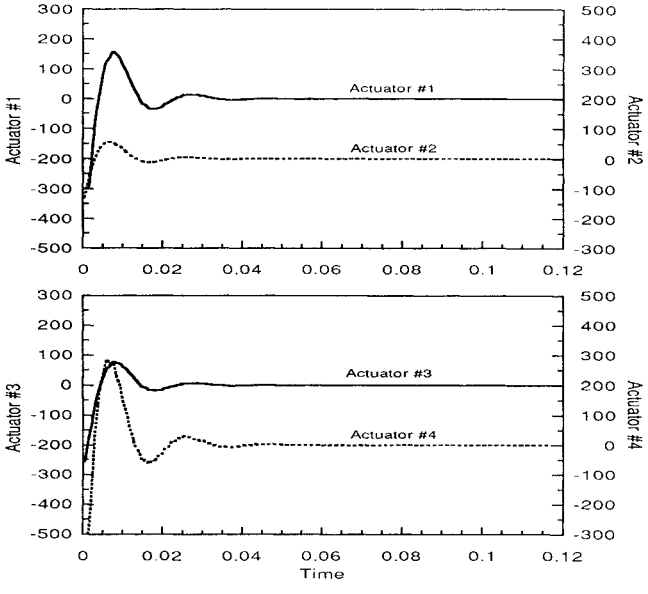

Fig. 12 Control voltages applied to the piezoelectric actuators of the optimized design.

and optimal actuators placement, respectively. The initial conditions $\{x_0\}$ are chosen arbitrarily. In these figures, the differences are hardly noticeable. It is because the closed-loop damping ratios of the dominant modes are very similar shown in Table 2. As shown in Table 2, first two closed damping ratios of each system are 0.352, 0.025 and 0.389, 0.029, respectively. However, the control input histories between the initial and optimal designs are noticeable. Figures 11 and 12 show the control voltages applied to the piezoactuators for each geometry. The figures show that the optimized geometry is more efficient. There is also a substantial saving in the control effort through the optimization process.

Conclusions

The main objective of this study is to design an active control system for flutter suppression of a composite wing using segmented piezoelectric actuators. The control system design, especially using optimal output feedback design, is performed for the active flutter suppression. For the aeroelastic control, the piezoelectric actuator must create substantial changes in surface shape to generate the aerodynamic loads. From piezoelectric parameters (location, size, and thickness), which affect the structural properties as well as the control characteristics, the thickness and size of the actuator are held constant. The optimization technique is applied to find the best locations of actuators for flutter control subject to minimize the control performance index. The results reveal the great potential of the piezoelectric materials to control flutter.

The closed-loop damping ratios are imposed so that the control system has more stability margin and, therefore, higher critical aeroelastic airspeed. However, heavy constraints on the damping ratio may result in higher gain matrix and more control efforts required for flutter suppression. As the optimization progresses, a tradeoff between the reduction of the performance index and satisfaction of constraints on the closed damping ratios is needed to determine the best locations of the piezoactuators. The results show the application of piezoactuators to the control of wing flutter and about a 49% increase in flutter speed compared with the open-loop configuration. Numerical results also show that a substantial savings in the control performance index is obtained from the optimization. In this paper, the power requirement has not been addressed. Future research will include the power requirement as well as the piezoelectric parameters, the ply orientation, and the thickness of the laminate.

References

[1]Crawley, E. F., and deLuis, J., "Use of Piezo-Ceramics as Distributed Actuators in Large Space Structures," *Proceedings of the 26th Structures, Structural Dynamics, and Material Conference*, AIAA, New York, 1985, pp. 126–133 (AIAA Paper 85-0626).

[2]Crawley, E. F., and deLuis, J., "Use of Piezoelectric Actuators as Elements of Intelligent Structures," *AIAA Journal*, Vol. 25, No. 10, 1987, pp. 1373–1385.

[3]Crawley, E. F., and Lazarus, K. B., "Induced Strain Actuation of Isotropic and Anisotropic Plates," *Proceedings of the 30th Structures, Structural Dynamics, and Material Conference*, AIAA, Washington, DC, 1989, pp. 1451–1461 (AIAA Paper 89-1326).

[4]Crawley, E. F., and Anderson, E. H., "Detailed Models of Piezoceramic Actuation of Beams," *Proceedings of the 30th Structures, Structural Dynamics, and Material Conference*, AIAA, Washington, DC, 1989, pp. 2000–2010 (AIAA Paper 89-1388).

[5]Wang, B., and Rogers, C. A., "Modeling of Finite-Length Spatially-Distributed Induced Strain Actuators for Laminate Beams and Plates," *Proceedings of the 32th Structures, Structural Dynamics, and Material Conference*, AIAA, Washington, DC, 1991, pp. 1511–1520 (AIAA Paper 91-1258).

[6]Ehlers, S. M., and Weisshaar, T. A., "Static Aeroelastic Behavior of an Adaptive Laminated Piezoelectric Composite Wing," *Proceedings of the 31st Structures, Structural Dynamics, and Material Conference*, AIAA, Washington, DC, 1990, pp. 1611–1623 (AIAA Paper 90-1078)

[7]Ehlers, S. M., and Weisshaar, T. A., "Effects of Adaptive Material Properties on Static Aeroelastic Control," *Proceedings of the 33rd Structures, Structural Dynamics, and Material Conference*, AIAA, Washington, DC, 1992, pp. 914–924 (AIAA Paper 92-2526).

[8]Crawley, E. F., Lazarus, K. B., and Bohlmann, J. D., "Static Aeroelastic Control Using Strain Actuated Adaptive Structures," *Proceedings of the First Joint U.S./Japan Conference on Adaptive Structures*, Technomic, Lancaster, PA, 1990, pp. 197–224.

[9]Lazarus, K. B., Crawley, E. F., and Lin, C. Y., "Fundamental Mechanisms of Aeroelastic Control with Control Surface and Strain Actuation," *Proceedings of the 32nd Structures, Structural Dynamics, and Material Conference*, AIAA, Washington, DC, 1991, pp. 1817–1831 (AIAA Paper 91-0985).

[10]Scott, R. C., and Weisshaar, T. A., "Controlling Panel Flutter Using Adaptive Materials," *Proceedings of the 32nd Structures, Structural Dynamics, and Material Conference*, AIAA, Washington, DC, 1991, pp. 2218–2229 (AIAA Paper 91-1067).

[11]Hajela, P., and Glowasky, R., "Application of Piezoelectric Elements in Supersonic Panel Flutter Suppression," AIAA Paper 91-3191, Sept. 1991.

[12]Heeg, J., "An Analytical and Experimental Investigation of Flutter Suppression Via Piezoelectric Actuators," *Proceedings of the AIAA Dynamics Specialist Conference*, AIAA, Washington, DC, 1992, pp. 237–247 (AIAA Paper 92-2106).

[13]Zeiler, T. A., and Weisshaar, T. A., "Integrated Aeroservoelastic Tailoring of Lifting Surfaces," *Journal of Aircraft*, Vol. 25, No. 1, 1988, pp. 76–83.

[14]Dracopoulos, T. N., and Öz, H., "Integrated Aeroelastic Control Optimization of Laminated Composite Lifting Surfaces," *Journal of Aircraft*, Vol. 29, No. 2, 1992, pp. 280–288.

[15]Jones, R. M., *Mechanics of Composite Materials*, Scripta, Washington, DC, 1975.

[16]Whitney, J. M., *Structural Analysis of Laminated Anisotropic Plates*, Technomic, Lancaster, PA, 1987.

[17]Albano, E., and Rodden, W. P., "A Doublet-Lattice Method for Calculating Lift Distributions on Oscillating Surfaces in Subsonic Flows," *AIAA Journal*, Vol. 7, No. 2, 1969, pp. 279–285.

[18]Karpel, M., "Design for Active Flutter Suppression and Gust Alleviation Using State-Space Aeroelastic Modeling," *Journal of Aircraft*, Vol. 19, No. 3, 1982, pp. 221–227.

[19]Hoadley, S. T., and Karpel, M., "Application of Aeroservoelastic Modeling Using Minimum-State Unsteady Aerodynamic Approximations," *Journal of Guidance, Control, and Dynamics*, Vol. 14, No. 6, 1991, pp. 1267–1276.

[20]Vanderplaats, G. N., *Numerical Optimization Techniques for Engineering Design with Application*, McGraw–Hill, New York, 1984.

[21]Levine, W. S., and Athans, M., "On the Determination of the Optimal Constant Output Feedback Gains for Linear Multivariable Systems," *IEEE Transactions on Automatic Control*, Vol. AC-15, No. 1, 1970, pp. 44–48.

[22]Moerder, D. D., and Calise, A. J., "Convergence of a Numerical Algorithm for Calculating Optimal Output Feedback Gains," *IEEE Transactions on Automatic Control*, Vol. AC-30, No. 9, 1985, pp. 900–903.

[23]Lewis, F. L., *Applied Optimal Control and Estimation*, Prentice–Hall, Englewood Cliffs, NJ, 1992.

[24]Mueller, G. S., and Adeniyi, V. O., "Optimal Output Feedback by Gradient Methods with Optimal Stepsize Adjustment," *Proceedings of the IEE, Control & Science*, Vol. 126, No. 10, 1979, pp. 1005–1007.

[25]Kailath, T., *Linear Systems*, Prentice–Hall, Englewood Cliffs, NJ, 1980.

[26]Chen, C. F., and Shieh, L. S., "A Note on Expanding $PA + A^TP = -Q$," *IEEE Transactions on Automatic Control*, Vol. AC-13, No. 2, 1968, pp. 122, 123.

[27]Bartels, R. H., and Stewart, G. W., "Algorithm 432: Solution of Matrix Equation $AX + XB = C$," *Communications of the ACM*, Vol. 15, No. 9, 1972, pp. 820–826.

[28]Kirk, D. E., *Optimal Control Theory*, Prentice–Hall, Englewood Cliffs, NJ, 1970.

[29]Vanderplaats, G. N., "ADS—A FORTRAN Program for Automated Design Synthesis, Version 1.10," Engineering Design Optimization, Inc., Santa Barbara, CA, May 1985.